TÜBİTAK

Turkish Journal of Botany

http://journals.tubitak.gov.tr/botany/

Research Article

Turk J Bot
(2014) 38: 851-863

doi:10.3906/bot-1311-8

Phytolith analysis of *Poa pratensis* (*Poaceae*) leaves

Zsuzsa LISZTES-SZABÓ[1,*], Szilvia KOVÁCS[1], Ákos PETŐ[2]

[1]Department of Agricultural Botany and Crop Physiology, Faculty of Agricultural and Food Sciences and Environmental Management, University of Debrecen, Debrecen, Hungary

[2]Hungarian National Museum, National Heritage Protection Center, Laboratory of Applied Research, Budapest, Hungary

Received: 06.11.2013 • **Accepted:** 01.04.2014 • **Published Online:** 15.08.2014 • **Printed:** 12.09.2014

Abstract: Phytoliths in *Poa pratensis* L. (Poaceae) leaf blades and sheaths are described in this study. The role of plant opal particles—known as phytoliths—is considerable in taxonomical studies, and their long-term preservation in sediments makes them a useful tool in the reconstruction of ancient plant communities and plant–human interactions. All together, 2244 phytoliths were counted and analyzed in 25 plant samples (5 shoots of 5 specimens and approximately 500–600 phytoliths per specimen). The biogenic silica content of *P. pratensis* leaves was determined at 2.61%, and 27 morphotypes have been described using the International Code for Phytolith Nomenclature. Two morphotypes are described for the first time in this study. Long cells (elongate psilate and sinuate morphotypes) and short cells (rondel–trapeziform elongated and rounded morphotypes) are frequently present in this species. Differences in morphotype frequency and significant differences in a few simple morphometric data (length, width, height) of long cells and short cells were found among specimens, which suggests that these features vary depending on environmental factors and the maturity of leaf tissues.

Key words: Biogenic silica, epidermis, phytolith, *Poa pratensis*

1. Introduction

Silica is considered an important factor for normal growth and development of plants (Agarie et al., 1996). Monosilicic acid is absorbed by plant roots from ground water and moves through the plant in the water-conducting xylem (Blackman and Parry, 1968). Many plant species subsequently deposit monosilicic acid as cell inclusions with a characteristic structure. These silica bodies (phytoliths) occur both over and between leaf veins and in the epidermis of inflorescence bracts or in culms and, in fewer cases, in the seeds as well.

Phenotypic plasticity of phytoliths induced by varying environmental conditions cannot obstruct the potential use of phytolith morphometries to discriminate between plant taxa. In some cases, when studying plant reference materials the shapes of silica bodies provided enough evidence for correct identification at species level (Lindstrom et al., 2000). Mejia-Saules and Bisby (2003) found taxonomically relevant silica bodies in lemmas of *Melica* L. species. The form and position of phytoliths, which are not greatly influenced by environmental factors but are genetically controlled, may have considerable systematic potential (Prychid et al., 2004). Genetic control of silica accumulation is emphasized by the phenomenon that domesticated wheat awns contained up to 19% silica per dry weight, as compared with 7% in wild accessions, suggesting a selection pressure associated with the domestication process (Peleg et al., 2010). The presence or absence of phytolith morphotypes as well as their abundance, proportion, and size can be an informative feature.

Silicified cells and silica bodies of plants are useful tools in archaeobotanical and paleoecological studies, because they are extremely durable in soil, may represent a potentially significant taxonomic character, and might indicate ancient environmental conditions and the physiological status of plants (For the latest comprehensive volume on the diversity of phytolith analyses see: Madella et al., 2012). Phytolith assemblage of species outside the European continent have been detailed in several studies (e.g., Papua New Guinea: Boyd et al., 1998; North America: Blinnikov et al., 2002; Canada: Boyd, 2005; South America: Zucol et al., 2005; Sri Lanka: Prematilake, 2006; Africa: Barboni et al., 2007; Asia: Strömberg et al., 2007, etc.); silica bodies of species in the flora of Europe have been studied to a lesser degree (Carnelli et al., 2004).

There is little information regarding detailed studies on the phytoliths of species in the Carpathian Basin; however,

* Correspondence: szabozs@agr.unideb.hu

descriptive studies of a few plant taxa—also other than grasses—do exist (Hodson et al., 1997; Sangster et al., 1997; Albert et al., 2011). Research of the kurgans, located on the Great Hungarian Plain, and reconstruction of the palaeoenvironments of their surroundings is necessary considering their natural and cultural value (Barczi et al., 2006, 2009). For this reason the aim of this study was to describe the phytolith assemblage of one of the dominant plant species of Pannonian grassland associations and habitats and to reveal its potential use in vegetation reconstruction.

Phytolith assemblages may play an important role in taxonomic separation among families, just like calcium oxalate styloids or starch grains, while tannins are also characteristic features in different families (Goldblatt et al., 1984; Rudall, 1994; Jafari et al., 2013). Epidermis micromorphology of different plant organs might provide useful tools for taxonomic recognition and separation (Mostafavi et al., 2013; Nassar et al., 2013). In order to identify species and genera and to use phytoliths as a taxonomic tool, it is necessary to understand morphological variations of phytolith assemblages within an individual plant and among individual specimens. This intention is in close relation with the phenomena of multiplicity and of redundancy, which in many cases hamper the direct linkage between phytolith morphotypes and plant taxa (Rovner and Russ, 1992). Since the same morphotype might be produced in different tissues of the same plant, and taxonomically related plants might produce similar morphotypes, it is necessary to understand the phytolith assemblage of different taxa.

To clear individual phytolith differences among specimens and to start describing phytolith assemblages of dominant grasses, *Poa pratensis* L. was chosen. With approximately 500 species, the meadow-grass (bluegrass) genus *Poa* L. is the largest genus in Poaceae (Clayton and Renvoize, 1986). It includes important turf and forage grasses (*Arrhenatheretea*: Soó, 1973; Borhidi, 2003) and cultivars, as well as troublesome weeds and invaders (Clayton and Renvoize, 1986). Although they are primarily found in the temperate zone, *Poa* is one of the most widely distributed grass genera (Hartley, 1961). Regarding the genus *Poa*, the *Poa pratensis* species group is one of the most taxonomically complicated groups in the world (Tutin et al., 1980). However, features of leaf epidermis and the presence and distribution of silicified unicellular hairs and prickles are useful characteristics for separating and identifying *Poa* species (Szabo et al., 2006).

Based on a preliminary study conducted on *Poa* specimens (Lisztes-Szabó et al., 2013) the aims of this study were:

(1) To provide further information on the possible phytolith assemblage differences among individuals of a species (in *Poa pratensis*, as a model plant), and

(2) to describe the phytolith assemblage of the lateral shoots in *Poa* species in the search for potentially indicative phytolith morphotypes, and

(3) to launch a reference material collection of the Carpathian Basin with the aim of comparing grass species and genera.

2. Materials and methods

Two *Poa pratensis* individuals from the *Poa* collection of the National Germplasm System of United States Department of Agriculture (USDA) were grown from grain and 3 *P. pratensis* specimens from the Herbarium of Debrecen University (HDU) were chosen for our study (Table 1). The specimens were selected from different countries with large geographical variation in order to represent different genetic backgrounds.

Lateral shoots (leaf blades and leaf sheaths; n = 5) were collected from each of the examined specimens at the end of their annual growing cycle. Five shoots of each specimen were compounded and treated as 1 sample. Phytolith extraction from the leaf blades and leaf sheaths was accomplished through dry ashing (Albert and Weiner, 2001) based on Mercader (2009, 2010). The mass of the leaves was weighed before and after drying, then the mass of the ash was weighed before and after adding a hydrochloric (HCl) and nitric acid (HNO_3) (1:1) solution

Table 1. Inventory of the examined *Poa pratensis* specimens and their biogenic silica content expressed in dry weight of the plant. Accession Nr. 1 and Nr. 2 are from the USDA collection, specimens Nr. 3–5 are from HDU, Hungary.

Specimen	Accession no.	Source	Original locality	Biogenic silica (%)
1	PI 227381 84i SD	Grain	Iran	1.84
2	PI 206725 84i SD	Grain	Turkey	6.92
3	Herbarium DU	Specimen	Hungary	0.86
4	Herbarium DU	Specimen	Czech Rep. (Brno)	1.06
5	Herbarium DU	Specimen	Czech Rep. (Olomouc)	2.37

followed by hydrogen peroxide (H_2O_2). After adding hydrogen peroxide, the samples were dried at 100 °C and weighed. The resulting mass was the biogenic silica content. The ashes were mixed thoroughly and mounted on light microscope slides in immersion oil and observed with a Zeiss Axioskop 2+ microscope at a magnification of 1000×.

Phytoliths (500–600 per specimen) were counted in adjacent but not overlapping lines across the cover slip (22 mm in width and length). Morphological classification was accomplished based on Twiss et al. (1969), while the denomination of individual morphotypes was accomplished according to the International Code for Phytolith Nomenclature 1.0 (ICPN 1.0; Madella et al., 2005). The classification and nomenclature work was complemented by the systems of other authors (Piperno and Pearsall, 1998; Blinnikov, 2005; Mercader et al., 2010; Blinnikov et al., 2011; Yost and Blinnikov, 2011; Honaine and Osterrieth, 2012). Within the most frequent morphotypes (as main types), subtypes were determined according to the ornaments of the silica bodies. Phytolith morphotypes were documented by microphotographs (Figures 1 and 2). The frequency of individual morphotypes was calculated, and results were visualized with the help of C2 ecological data visualization software (Juggins, 2007). The ubiquity of morphotypes was noted.

The longest parameter of the forms (length) was measured, which means a parallel measuring to the fore axis of the leaf in most cases. The width of forms was measured in the middle of the silica body perpendicular to the beam. In 4 phytolith morphotypes (elongated, keeled, rounded, and pyramidal rondels) the sides of the silica body could be identified and, subsequently, their heights measured. The heights of these cells equal the thickness of the epidermis at that point. Up to 70 phytoliths were measured by ImageJ 1.32j software (Abramoff et al., 2004) and described by mean values, standard deviation, and minimum and maximum values (descriptive statistics). Width, length, and height data of the 2 most frequent morphotypes were analyzed by one-way analysis of variance (ANOVA) using SigmaPlot 11.0 software (Systat Software, San Jose, CA, USA) to identify significant differences among specimens.

3. Results

3.1. Descriptive results of *Poa pratensis* lateral shoot phytoliths

The ash of the *Poa pratensis* shoots contained fully silicified silica bodies, cells with silicified walls, corroded silicified cells, and debris of silicified cell walls, as well as parts of epidermis tissue. The average silica content was 2.61% of plant dry weight (range: 0.86%–6.92%; standard deviation: 2.48) in the *P. pratensis* shoots (Table 1). Specimen Nr. 2 contained a prominently higher amount of biogenic silica; its content was more than 2-times higher than the average value.

Approximately 500–600 photographs were taken of each specimen for a total of 1001 (149–257 per specimen) classified and a total of 1154 (150–431 per specimen) unclassified phytoliths. All together, 2244 phytoliths were counted. Several (79) tissue photographs were taken because the ash contained cells that adhered to each other (cf. silica sheet elements). In this study, 27 well-defined morphotypes are reviewed as these may bear taxonomical properties. Two morphotypes, considered to be new, were also described. In addition to the descriptor list provided by ICPN 1.0, new descriptors were added to denominate all observed morphotypes of *Poa pratensis* (Table 2). Table 2 and Figure 3 provide a summary of the observed features of *P. pratensis* phytolith assemblage.

Table 3 gives an overview of the morphotype frequencies of the 2 most frequent morphotype groups: the elongates and the rondel–trapeziforms. Based on the experimental data, the proportion of elongate morphotypes varied between 44.1% and 76.6%, which represents great individual variability within the same species. The most frequent elongate morphotypes were the psilate, the sinuate, and the so-called unclassified (which could not be classified into any exact category). The highest diversity of elongate morphotypes was found in specimen Nr. 5 (Table 3). This implies 8 morphotypes that have 8 different ornaments. The examination of specimen Nr. 2 resulted in the fewest subtypes (4) (Table 3).

The results show that the frequency of the rondel–trapeziform morphotype group varied on a broad scale between 9.3% and 46.1% (Table 3). The elongated and rounded subtypes were the most frequent in 4 specimens out of the examined 5 (Table 3). The pyramidal and keeled subtypes were among the 3 most frequent types, as well. The highest diversity of rondel–trapeziform morphotype group was found in specimen Nr. 1, which contained all 6 described morphotypes. Specimens Nr. 2 and Nr. 5 yielded the fewest morphotypes (4) (Table 3).

In several cases small, square tabulars were observed (Figure 2F) within the elongate forms and, in a few cases, in the rondels (Figure 1Od). The presence of these freestanding, square tabulars (1–3 μm) could also derive from the dry ashing procedure, during which they were liberated from the cells and freely appeared in the ash.

3.2. Catalogue of the studied morphotypes

Table 2 gives a summary of the detailed descriptions of the studied phytoliths of *Poa pratensis* leaves. However, we felt it necessary to more precisely describe a few morphotypes. Their description is appended below:

Elongate morphotype group: Much longer than wide forms (ICPN 1.0); most often with inclusions (Figures

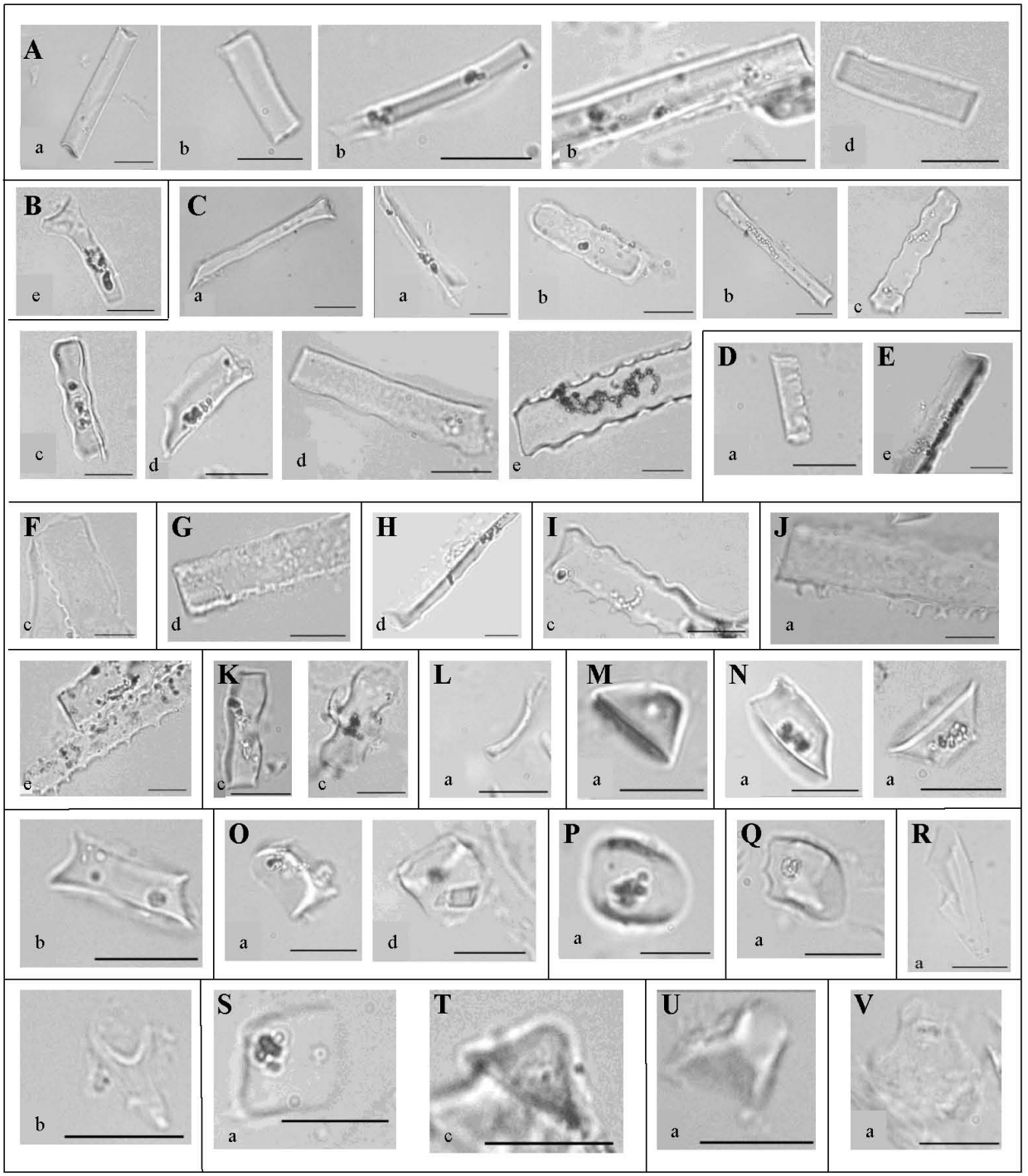

Figure 1. *Poa pratensis* leaf phytolith micrographs. A- elongate psilate forms with different termination, B- elongate other, C- elongate sinuate, D- elongate verrucate, E- elongate castellate, F- elongate crenate, G- elongate lacunose, H- elongate pileate, I- elongate corniculate, J- elongate echinate (a- with little branches), K- elongate lobate, L- elongate depressed, contorted, M- rondel-trapeziform pyramidal depressed, N- rondel-trapeziform elongated, O- rondel-trapeziform keeled (d- with small tabular), P- rondel-trapeziform rounded, Q- rondel-trapeziform horned, R- prickle, S- tabular psilate, T- papilla, U- parallelepipedal bulliform, and T- cuneiform bulliform. Scale bar = 10 µm. Specimen: a- 1, b- 2, c- 3, d- 4, e- 5.

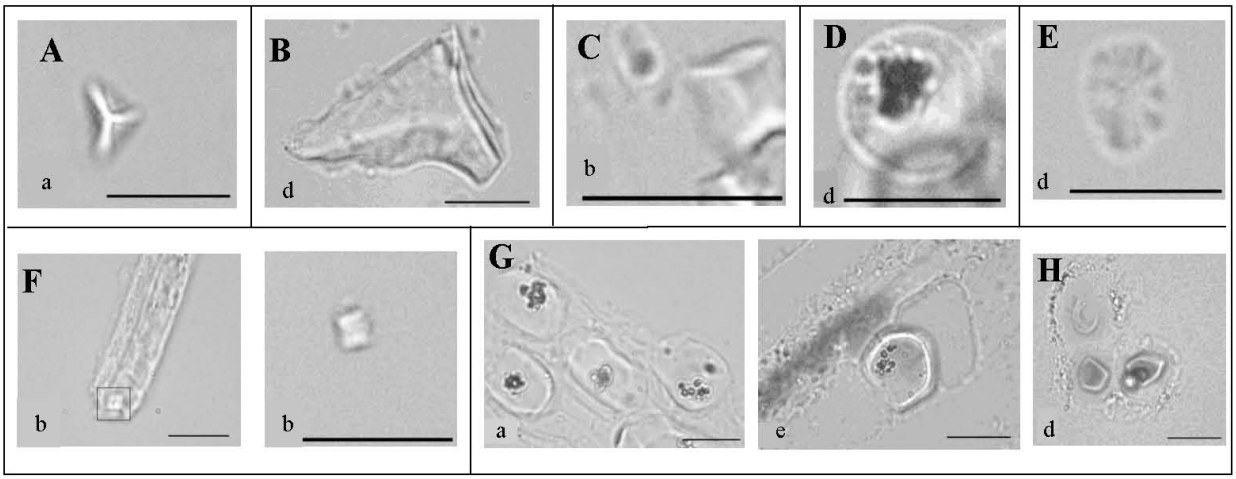

Figure 2. *Poa pratensis* leaf phytolith micrographs. A- trigonal pyramid psilate, B- scutiform, C- cubic psilate, D- globular, E- stellate laminate, F- elongate form with small tabular, G- tissue fragments (a. silica bodies of the costal zone, e. silica body of the intercostal zone), H- corroded short cells. Scale bar = 10 µm. Specimen: a- 1, b- 2, c- 3, d- 4, e- 5.

1A–L). This group is the most frequent type (58.6%) (Table 2) in the examined specimens; they represent the elongate cell of the epidermis. There is a great variability within the shape, length, and thickness of the elongate cells. Their proportion within the specimen varies (44.1%–76.6%) (Table 3). The ends of the long cells can be concave, convex, or asymmetrical, acute, obtuse, or linear. We divided this morphotype to more subtypes based on the second descriptor of ICPN 1.0, which concerns texture and ornamentation. Other, less well-defined elongated cells were collected into a group called unclassified elongate (Figure 1B). These cells do not have well-characterized geometrical shape or ornaments. Their frequency was 14.6% within the whole assemblage (Table 2), and varied between 9.6% and 40.4% within the studied specimens (Table 3). The elongate cells are mainly from the long cells of the epidermis, and these types were observed in all specimens (ubiquity was 5). The proportion of the elongate psilate phytoliths is half of that of the elongate forms. This morphotype was found frequently in the costal epidermis region alternating with rounded or elongated rondels.

Elongate depressed, contorted, and psilate: Elongate, narrow, and flat form without inclusions. The morphotype probably derives from the epidermis (Figure 1L). Its frequency was 0.7% (Table 2), and it varied between 0.5% and 4.3% within the elongate morphotype assemblage (Table 3). This morphotype was observed in 3 specimens (U = 0.6) (Table 2). To our knowledge similar morphotypes were not previously described.

Rondel–trapeziform morphotype group: Contracted morphotype group indicated with the nomina conservanda rondel and the descriptor of trapeziform (ICPN 1.0). These phytoliths are the short cells of the epidermis. Inclusions were observed within these silica bodies. These forms have the outline of a trapezoid, an incomplete pyramid or pyramid, and intermediate forms of these in a side view (Figures 1M–Q). They show rectangular, oblong, oval, rounded, or intermediate forms in top view and bottom view and concave or straight sides in side view. According to our experience, the costal epidermis of blue meadow grass has cell rows that are richer in rondel–trapeziforms (Figure 2Ga) than the intercostal zone (Figure 2 Ge). The frequency of this morphotype group was 27.7% (Table 2). Its frequency varied between 9.3% and 46.1% (Table 3) and was observed in all 5 specimens, which results in a ubiquity value of 1.0 (Table 2).

Lanceolate trichome (prickle): Curvate unicellular hair (ICPN 1.0) (Figure 1R). Only a few trichomes were observed. The base of the trichomes was less silicified than the apex; therefore the more resistant apex part of the trichome could have been observed more frequently in the recovered ash material. The frequency was 2.3% (Table 2). This morphotype was detected in all specimens (U = 1.0) (Table 2).

Papilla: Low conical or pyramidal forms without inclusions (ICPN 1.0; nomina conservanda) (Figure 1T). The frequency of epidermal papillae was 1.9% (Table 2). This morphotype was detected in all specimens (U = 1.0) (Table 2).

Bulliform cells: A few, principally cuneiform bulliform or parallelepipedal bulliform (also called blocky; Blinnikov, 2005) cells were observed (ICPN 1.0) (Figures 1U–V). The morphotypes did not show any signs of inclusions. Due to their thin cell walls, these cell types are not as resistant as the epidermal cells, and they could have been corroded during the dry ashing procedure. The frequency was 2.4%

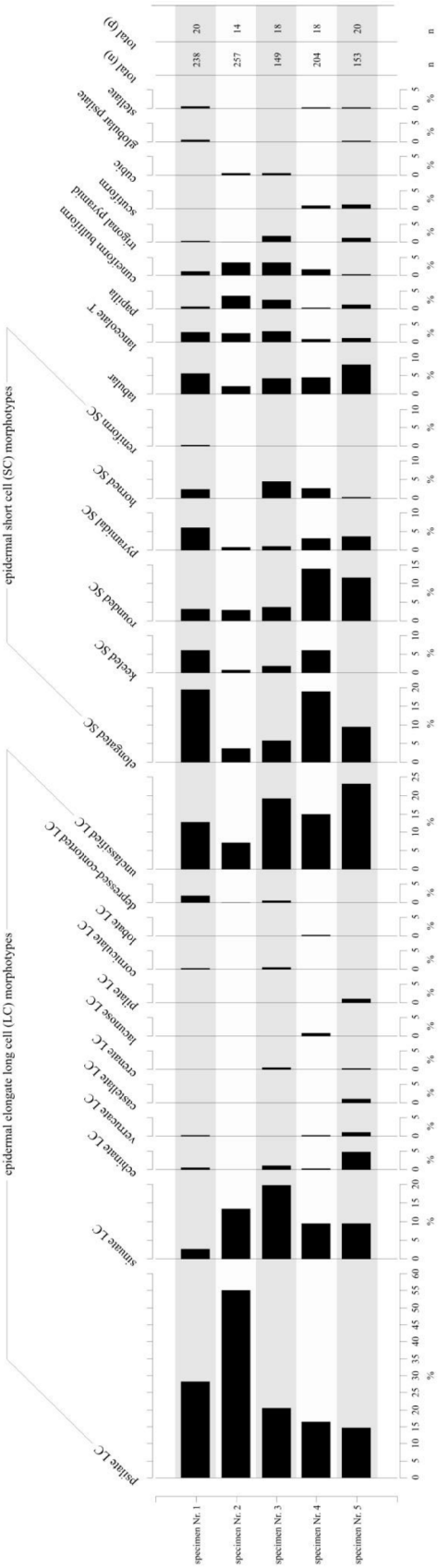

Figure 3. Phytolith morphotype distribution in *Poa pratensis* lateral shoots.

Table 2. Distribution of phytolith morphotypes in the examined shoots of *Poa pratensis* specimens: denominate code of morphotypes (N) and figure number, descriptors, presence in specimen, references; ubiquity: presence of morphotypes in specimen, total (n), frequency (%) in the classified phytolith assemblage of the 5 specimens.

N	Fig.	First descriptor	Second descriptor	Characteristics, reference for descriptors	Presence in specimen	Ubiquity	n	%
	1A-L	Elongate		ICPN	12345	1.0	587	58.6
1	1A	Elongate	Psilate	Elongated form without well-defined ornaments or texture (ICPN)	12345	1.0	298	29.8
2	1B	Elongate	Unclassified	Forms without well-defined shape; or phytolith fragments, as well as silicified cell wall fragments (this study)	12345	1.0	146	14.6
3	1C	Elongate	Sinuate	Having a margin with alternating but uneven concavities and convexities (ICPN)	12345	1.0	108	10.7
4	1J	Elongate	Echinate	Ornamented with prickles (ICPN)	1 345	0.8	13	1.3
5	1D	Elongate	Verrucate	Long form with irregularly shaped, wart-like processes (ICPN)	1 45	0.6	4	0.4
6	1E	Elongate	Castellate	Having square to rectangular processes (ICPN)	5	0.2	2	0.2
7	1F	Elongate	Crenate	Notched or scalloped, dented with the teeth rounded (ICPN)	3 5	0.4	2	0.2
8	1G	Elongate	Lacunose	Pitted and marked with small depressions (ICPN)	4	0.2	2	0.2
9	1H	Elongate	Pileate	Having rod-like processes with concave sides (ICPN)	5	0.2	2	0.2
10	1I	Elongate	Corniculate	Having horn-like projections (ICPN)	3	0.2	2	0.2
11	1K	Elongate lobate	Psilate	Elongated form with lobes (ICPN)	4	0.2	1	0.1
12	1L	Elongate depressed	Psilate	Elongate, narrow and flat form without inclusions (this study)	123	0.6	7	0.7
	1M-Q	Rondel–trapeziform		ICPN	12345	1.0	277	27.7
13	1N	Rondel–trapeziform	Elongated	Trapeziform in side view, oblong to oval in top view (Blinnikov, 2005)	12345	1.0	120	12.0
14	1O	Rondel–trapeziform	Keeled	Short cell without surface in top view, prism with 3 rectangular and 2 triangular sides (modified after Blinnikov, 2005)	1234	0.8	34	3.4
15	1P	Rondel–trapeziform	Rounded	So-called pure rondel form with orbicular surface in top and bottom view (ICPN)	12345	1.0	69	6.9
16	1M	Rondel–trapeziform	Pyramidal	Short cell morphotype with quadrilateral base and pointed top (Blinnikov, 2005)	12345	1.0	33	3.3
17	1Q	Rondel–trapeziform	Horned	Trapeziform in side view, oval or reniform in top view, with horned-like protrusions (Blinnikov, 2005)	1 345	0.8	20	2.0
18		Rondel–trapeziform	Reniform	Rondel form, kidney-shaped in 2-D top view (ICPN)	1	1.0	1	0.1
19	1S	Tabular	Psilate	Thin and table-like with or without inclusions, having different size and origin (ICPN)	12345	1.0	50	5.0
20	1R	Lanceolate trichome	Psilate	Curvate unicellular hair (prickle) (ICPN)	12345	1.0	23	2.3

Table 2. (Continued).

N	Fig.	First descriptor	Second descriptor	Characteristics, reference for descriptors	Presence in specimen	Ubiquity	n	%
21	1T	Papilla	Psilate	Low conical or pyramidal forms without inclusions (ICPN)	12345	1.0	19	1.9
22	1U-V	Bulliform	Psilate	Cuneiform bulliform or parallelepipedal bulliform (also called blocky; Blinnikov, 2005) (ICPN)	12345	1.0	24	2.4
23	2A	Trigonal pyramid	Psilate	Triangular in side view and bottom view with an apex (this study)	123 5	0.8	7	0.7
24	2B	Scutiform	Psilate	Shield shaped (ICPN)	45	0.4	4	0.4
25	2C	Cubic	Psilate	An epidermal short cell form with 6 equal square sides (ICPN)	23	0.4	3	0.3
26	2D	Globular	Psilate	Spherical with central perforations (ICPN)	1 5	0.4	3	0.3
27	2E	Stellate	Laminate	Star shaped with laminate surface (ICPN)	1 45	0.6	4	0.4
		Classified		Forms with well-defined shape and/or ornaments			1001	49.6
	2H	Corroded		Corroded silica bodies, silicified cells and cell fragments	12345	1.0	89	7.8
		Unclassified		Forms without well-defined shape and/or ornaments	12345	1.0	1154	50.4

(Table 2). This morphotype was detected in all specimens (U = 1.0) (Table 2).

Trigonal pyramid: These morphotypes are triangular in side view and bottom view with an apex (Figure 2A). The frequency of the morphotype was 0.7% (Table 2). This morphotype was detected in 4 specimens (U = 0.8) (Table 2).

Scutiform: Shield shaped morphotype, probably trichome (ICPN 1.0) (Figure 2B). Its frequency was 0.4%, and it gave a ubiquity value of 0.4 (Table 2).

Corroded: Corroded silica bodies, silicified cells, and cell fragments were also observed. Silicified cells may have been corroded by the acid treatment that was applied during the recovery procedure; however, the structure of the cell was often recognized (for an example, see Figure 2H). The frequency of these forms was 7.1% within the total phytolith assemblage (Table 2). Since they were observed in all specimens, their ubiquity value is 1.0 (Table 2).

3.3. Results of morphometric measurements

The morphometric characteristics of the examined morphotypes are summarized in Table 4. The average length of elongate long-cell morphotypes was 19.8–45.4 µm, while the average width was between 1.9 and 13.3 µm. The average length of rondel short cell was 4.9–13.0 µm, while the average width was 7.2–9.3 µm. Length and width of tabulars and measured data of stellate phytoliths are similar to those of rondel–trapeziform short cells. The widest base of trichomes is 11.9 µm, but these are usually broken in the ash so their length could not be identified. The average width of papillae is 4.1 µm. As expected, bulliforms had a larger size than short cells, and their average length was 10.3–11.5 µm and average width 14.7–17 µm. The smallest observed phytoliths were trigonal pyramids (3.1–3.3 µm) and cubic short cells (3.5 µm).

The sizes of the different morphotypes were significantly different among the individual specimens. In the most frequent types, elongate unclassified and elongate sinuate morphotypes had significant differences in width and length among *Poa pratensis* specimens; however, elongate psilate cells differ only in width, while their length did not vary significantly (Table 4). The width of rondel–trapeziform elongated, keeled, rounded, and horned types differ from each other significantly among the specimens, but the length and the height data do not (with the exception of height in the elongate type). A significant difference was not found among rondel–trapeziform pyramidal phytoliths.

4. Discussion

The average biogenic silica content of the studied specimens of C_3 grass *Poa pratensis* was 2.61%. This value matches the average of 26 Poaceae species earlier

Table 3. Frequency (%) of elongate and rondel–trapeziform phytoliths in *Poa pratensis* shoots. Elongate and rondel–trapeziform frequencies are in proportion of classified phytoliths, and the subtypes are in the proportion of the main morphotypes.

Morphotype		Specimen (%)				
		Nr. 1	Nr. 2	Nr. 3	Nr. 4	Nr. 5
Elongate		**48.3**	**76.6**	**64.4**	**44.1**	**58.2**
	Psilate	59.1	72.0	32.3	37.7	25.8
	Unclassified	26.9	9.6	30.2	34.4	40.4
	Sinuate	6.0	17.8	32.3	22.2	16.8
	Echinate	1.7	-	2.1	1.1	9.0
	Verrucate	0.9	-	-	1.1	2.2
	Castellate	-	-	-	-	2.2
	Crenate	-	-	1.0	-	1.1
	Lacunose	-	-	-	2.2	-
	Pileate	-	-	-	-	2.2
	Corniculate	0.9	-	1.0	-	-
	Lobate	-	-	-	1.1	
	Depressed	4.3	0.5	1.0	-	-
Rondel–trapeziform		**38.7**	**9.3**	**18.1**	**46.1**	**26.1**
	Elongated	51.0	41.6	33.3	41.5	37.5
	Keeled	16.3	12.5	11.1	13.8	-
	Rounded	8.7	33.3	22.2	30.8	45.0
	Pyramidal	16.3	12.5	7.4	7.4	15.0
	Horned	6.5	-	25.9	6.4	2.5
	Reniform	1.0	-	-	-	-

studied by Mercader et al. (2010). They found a wide range of average biogenic silica content in grass species and determined average biogenic silica content at 4.59% (Niassa Rift, Mozambique) (range: 0.66%–23.30%). In this study, specimen Nr. 2 showed prominently high biogenic silica content, and it had high elongate sinuate long cell content as well. In the present study the propagulum of specimen Nr. 2 was grown under the same conditions as specimen Nr. 1; therefore the difference in biogenic silica content is likely related to the genetic background of silica accumulation.

To characterize phytolith assemblages of plant species, 3 important aspects must be considered: the variation of morphotypes (descriptive results), interspecific frequency, and morphometric data. Concerning the first and second aspects, *P. pratensis* shoots (leaf blades and sheaths) accumulate silica in their epidermal cells, in both short and long cells, as this feature is typical in most *Poales* (Metcalfe, 1960; Prychid et al., 2004).

Variation of morphotypes: Due to size and ornamentation properties, there are several forms of short and long silica bodies. Blinnikov et al. (2013) also showed several rondels and plates in blue meadow grass in grasslands of controlled composition on experimental plots (Cedar Creek, Minnesota, USA). The proportion of long, psilate cells was 29.8% in this study, while Morris et al. (2009) found only 16% of these morphotypes in blue meadow grass individuals in their study. Similarly, a high proportion of elongate morphotypes was found by Morris et al. (2009) in *Poa secunda* Presl and by Blinnikov (2005) in *P. sandbergii* Vasey. Morris et al. (2009) mentioned elongate forms with mostly squared ends, which correlates

Table 4. The number of measured *Poa pratensis* shoot phytoliths and descriptive statistics of the morphometrical data. Rt: rondel–trapeziform, b: bulliform. Individual type names are without second descriptors. *: significant differences among specimen; #: not significant (α = 0.05).

Morphotypes	Number of measured phytoliths					Width mean	SD	Min	Max	Length mean	SD	Min	Max	Height mean	SD	Min	Max
	1	2	3	4	5												
E psilate	68	70	31	34	23	***5.1**	2.9	0.8	17.5	**#25.1**	10.9	7.3	56.1				
E unclassified	31	19	29	31	36	***6.8**	4.1	1.6	18.5	***20.7**	10.7	5.6	47.3				
E sinuate	7	35	31	20	15	***6.6**	2.6	1.4	13.6	***31.3**	10.5	11.3	53.2				
E echinate	2		2	1	8	**10.8**	3.5	6.3	18.1	**31.0**	15.9	14.6	46.3				
E verrucate	1			1	2	**9.0**	4.2	4.0	12.7	**35.3**	20.3	13.8	55.1				
E castellate					2	**8.3**	0.6	7.9	8.7	**30.2**	18.3	17.2	43.2				
E crenate			1		1	**13.3**	0.1	13.3	13.4								
E lacunose				2		**9.5**	0.2	9.4	9.6	**42.9**	5.7	38.9	46.9				
E pileate					2	**6.5**	0.1	6.4	6.5								
E corniculate	1		1			**8.0**				**45.4**							
E lobate					1	**7.2**				**20.2**							
E depressed	5	1	1			**1.9**	0.6	1.4	3.3	**19.8**	10.4	10.6	35.6				
Rt elongated	47	10	9	39	15	***5.0**	2.4	1.0	11.3	**#13.0**	3.5	3.2	20.5	***3.5**	1.6	0.8	8.1
Rt keeled	13	3	3	13		***7.2**	3.3	2.2	15.2	**#10.2**	2.9	4.9	15.6	**#3.8**	1.4	1.9	6.9
Rt rounded	5	8	6	29	18	***9.3**	2.5	5.0	18.2	**4.9**	2.2	3.2	8.7	**#4.0**	1.5	1.4	8.5
Rt pyramidal	15	3	2	7	6	**#7.8**	3.7	3.1	16.7					**#4.7**	2.0	1.0	9.0
Rt horned	6		7	6	1	***8.5**	2.6	4.0	13.1								
Rt reniform	1					**7.3**				**9.9**							
Tabular	14	6	7	10	13	**6.7**	3.2	2.2	17.4	**8.7**	3.9	3.8	23.0				
Trichome	7	7	5	2	2	**11.9**	7.5	2.0	32.2								
Papilla	2	10	4	1	2	**4.1**	1.8	2.1	8.9								
Parallelepipedal b.	2	7	3	0	2	**10.3**	6.8	2.8	23.0	**17.0**	10.4	4.5	39.8				
Cuneiform b.	1	3	3	2	2	**11.5**	5.2	5.8	24.2	**14.7**	8.1	6.0	25.4				
Trigonal pyramid	1	1	3		2	**3.3**	1.1	1.9	5.1	**3.1**	1.0	2.2	4.8				
Cubic		2	1			**3.5**	1.8	2.0	5.6								
Stellate	2			1	1	**8.8**	2.7	7.4	12.9								

with our findings, although lower production of horned (2.0%) and keeled (3.4%) rondel types was observed than in Morris et al. (2009). They found that *P. pratensis* stood out from the other grasses with its high production of both horned (23%) and keeled (19%) rondel types. It is not surprising that the frequency of these morphotypes in samples from the present study differs in part from *Poa* sp. or *P. pratensis* data of other sources, because specimens in this study also vary among each other measurably.

There is a diverse range of silica body shapes in Poaceae including dumbbell-shaped and cross-shaped intermediates between these 2 types, horizontally elongated shapes with psilate or sinuous outlines, saddle-shaped, conical-shaped, and numerous others (Metcalfe, 1960; Ponzi and Pizzolongo, 2003; Prychid et al., 2004). It is interesting to note that similar to the results in Brown (1984b), cross-shaped and saddle-shaped forms were absent in the examined *Poa pratensis* shoots. Only a few prickles (unicellular trichomes), and especially their peaks, could be observed, because long, multicellular trichomes are not typical in this species (Metcalfe, 1960). However, it is also true that the silica content is higher in the apex of the prickles than in their base; therefore the recovery and observation of apex fragments has higher probability.

In general, the bulliform frequency was low. Silica content of bulliforms is generally less than that of the other cells located in the epidermis. This difference can probably be explained by the function of bulliform cells. Their responsibility is to change the cell lumen by changing the flexibility of the cell wall and to help the leaf convolve up under arid conditions (Abernethy et al., 1998; Nawazish et al., 2006). Similar to Morris et al. (2009), only scarce amounts of bulliforms, bilobates, and papillae were found, although their analysis was based on only 119 phytolith particles in contrast to the 2244 pieces analyzed in the present study.

Two phytolith types were newly described during the examination of *P. pratensis* leaves. These morphotypes were the following:

(i) Elongate depressed and contorted (1.9–19.8 µm), which was present in 3 specimens, and

(ii) trigonal pyramid (3.1–3.3 µm), which was present in 4 specimens although with low frequency values.

The elongate unclassified group has been created by the current authors. Morphotypes classified in this category were present in all examined specimens with high frequency, and in our view they represent nondiagnostic silica bodies. The corroded forms refer to the fact that acids during the dry ashing procedure may injure silica bodies and silicified cell walls.

Interspecific frequency: Similarly to the conclusions in Brown (1984a), interspecific variation could be observed in this sample set. Not all shapes common to a given species were found in every specimen. Some were not found at all. Genetic variation among plants and geographic location may cause intraspecific differences in phytolith assemblages (Mulholland et al., 1988, 1990). Additionally, in connection with phytolith morphotype differences among taxa the examples above underline the fact that taxonomical value of the presence or absence of a phytolith morphotype is important, but to evaluate them one should have proper knowledge of intraspecific variations.

Morphometric characters: Considering the third aspect, the size of the different morphotypes may also be significantly different among individuals. Elongate long-cell morphotypes of *Poa pratensis* leaves are larger than medium sized (>20 µm; Mercader et al., 2010). The average length (or diameter) of rondel–trapeziform short cells was between 4.9 and 13.0 µm, and the average width was 7.2–9.3 µm. These were shorter than the short cells in the grasses of the European Alps studied by Carnelli et al. (2004). In the aforementioned study Carnelli et al. (2004) found that these values vary between 15 and 30 µm. Brown (1984a, 1984b) demonstrated that a direct relationship between moisture and phytolith size appears. Size differences within subfamilies are apparent. Piperno and Pearsall (1998) found that many bilobates isolated from panicoid grasses exceeded 20 µm in length, whereas those from the Bambusoideae, Chloridoideae, and Pooideae (with the exception of *Stipa*) were almost without exception shorter. Portillo et al. (2006) found that *Avena sativa* L. and *Avena strigosa* Schreb taxa produced the same types of phytoliths, although those phytoliths had significantly different size parameters.

Based on the morphometric measurements performed on *P. pratensis* specimens it is suggested that interspecific differences do not only exist in terms of difference in frequency, but also as size variation.

Additional consequences: Brown (1984a, 1984b) and Mulholland (1989) carried out more extensive studies of North American grasses and found that although the 3-part division described by Twiss et al. (1969) could generally be upheld, there were significant deviations from the expected pattern. The same was true of the tropical grasses studied by Piperno and Pearsall (1998). This 3-part division seems to be relevant for *Poa pratensis* shoots, because frequencies of saddle (typical of Panicoideae) and bilobate (typical of Chloridoideae) were low (only 1 lobate was found in this study), but circular/oval rectangular (in present study: rondel–trapeziform) frequency was high (typical of Pooideae). Although studied specimens of *Poa pratensis* were from wet grasslands, because *P. pratensis* is restricted to wet, cool areas in Europe, Asia, and the Pacific Northwest (Monsen et al., 2004), microhabitat factors may have an effect on frequency and size of phytolith

morphotypes. Furthermore, we cannot exclude the phenomenon of an individual plant yielding a significantly different amount of silica with ageing. The stage of plant maturity may influence biogenic silica accumulation and, in consequence, intraspecific variation as well (Hodson et al., 1985). The latter may also cause a wide range of variation in phytolith morphotype proportions within the specimen.

Due to the fact that the dry ashing procedure may produce numerous secondary products that appear in a free state or within on the cell wall, it is difficult to study the ultrastructure of a silicified cell wall. Similar to the findings in Wilding et al. (1977), the small-sized (1–3 μm), square tabulars that were observed in this study may be parts of the cell ultrastructure or, alternatively, may represent secondary products. These pieces were observed in several elongate types with thin cell walls, but in only 1 specimen in rondels (Nr. 4).

Final conclusion: Through detailed morphological analyses this study not only provides taxonomically relevant data on phytolith assemblage of *P. pratensis* and the palaeophytogeography of the grasslands, but also reveals that intraspecific variance of frequency and size exists within the phytolith assemblage of the same species. Hopefully the latter finding will help prevent the making of inappropriate taxonomic inferences from phytoliths.

References

Abernethy GA, Fountain DW, McManus MT (1998). Observations on the leaf anatomy of Festuca novae-zelandiae and biochemical responses to a water deficit. New Zeal J Bot 36: 113–123.

Abramoff MD, Magalhaes PJ, Ram SJ (2004). Image processing with ImageJ. Biophot Int 11: 36–42.

Agarie S, Agata W, Uchida H, Kubota F, Kaufman P (1996). Function of silica bodies in the epidermal system of rice (*Oryza sativa* L.): testing the window hypothesis. J Exp Bot 47: 655–660.

Albert RM, Esteve X, Portillo M, Rodriguez-Cintas A, Cabanes D, Esteban I, Hernandez F (2011). Phytolith CoRe, phytolith reference collection. Website: http://www.gepeg.org/enter_PCORE.html [accessed 20 July 2012]

Albert RM, Weiner S (2001). Study of opal phytoliths in prehistoric ash layers using a quantitative approach. In: Meunier J, Coline F, editors. Phytoliths: Applications in Earth Sciences and Human History. Lisse, Netherlands: Balkema, pp. 251–266.

Barboni D, Bremond L, Bonnefille R (2007). Comparative study of modern phytolith assemblages from inter-tropical Africa. Palgeog Palclim Palecol 246: 454–470.

Barczi A, Tóth TM, Csanádi A, Sümegi P, Czinkota I (2006). Reconstruction of the paleo-environment and soil evolution of the Csípő-halom kurgan, Hungary. Quat Int 156: 49–59.

Barczi A, Golyeva AA, Pető Á (2009). Palaeoenvironmental reconstruction of Hungarian kurgans on the basis of the examination of palaeosoils and phytolith analysis. Quatern Int 193: 49–60.

Blackman E, Parry DW (1968). Opaline silica bodies in the range grasses of southern Alberta. Can J Bot 49: 769–781.

Blinnikov M, Busacca A, Whitlock C (2002). Reconstruction of the late Pleistocene grassland of the Columbia Basin, Washington, USA, based on phytolith records in loess. Palgeog Palclim Palecol 177: 77–101.

Blinnikov MS (2005). Phytoliths in plants and soils of the interior Pacific Northwest, USA. Rev Palaeobot Palyno 135: 71–98.

Blinnikov MS, Bagent CM, Reyerson PE (2013). Phytolith assemblages and opal concentrations from modern soils differentiate temperate grasslands of controlled composition on experimental plots at Cedar Creek, Minnesota. Quatern Int 287: 101–113.

Blinnikov MS, Gaglioti BV, Walker DA, Wooller MJ, Zazula GD (2011). Pleistocene graminoid-dominated ecosystems in the Arctic. Quatern Sci Rev 30: 2906–2929.

Borhidi A (2003). Magyarország növénytársulásai. Budapest, Hungary: Akadémiai Kiadó (in Hungarian).

Boyd M (2005). Phytoliths as paleoenvironmental indicators in a dune field on the northern Great Plains. J Arid Environ 61: 357–375.

Brown DA (1984a). Prospects and limits of a phytolith key for grasses in the Central United States. J Archaeol Sci 11: 221–243.

Brown DA (1984b). Prospects and limits of a phytolith key for grasses in the Central United States. J Archaeol Sci 11: 345–368.

Carnelli AL, Theurillat J-P, Madella M (2004). Phytolith types and type-frequencies in subalpine–alpine plant species of the European Alps. Rev Palaeobot Palyno 129: 39–65.

Clayton WD, Renvoize SA (1986). *Genera Graminum*: Grasses of the World. Kew Bull. Additional Series XIII. London, UK: Royal Botanic Gardens.

De Melo SP, Monteiro FA, De Bona FD (2010). Silicon distribution and accumulation in shoot tissue of the tropical forage grass *Brachiaria brizantha*. Plant and Soil 336: 241–249.

Goldblatt P, Henrich JE, Rudall P (1984). Occurrence of crystals in *Iridaceae* and allied families and their phylogenetic significance. Ann Missouri Bot Gard 71: 1013–1020.

Hartley W (1961). Studies on the origin, evolution, and distribution of the Gramineae. IV. The genus *Poa* L. Aust J Bot 9: 152–161.

Hodson MG, Sangster AG, Parry DW (1985). An ultrastructural study on the developmental phases and silification of the glumes of *Phalaris canariensis* L. Ann Bot-London 55: 649–665.

Hodson MJ, Williams SE, Sangster AG (1997). Silica deposition in the needles of the Gymnosperms. I. Chemical analysis and light microscopy. In: Pinilla A, Juan-Tresserras J, Machado MJ, editors. The state-of-the-art of phytoliths in soils and plants. Centro de Ciencas Medioambientales. CSIC Monograf 4: 135–146.

Honaine MF, Osterrieth ML (2012). Silification of the adaxial epidermis of leaves of panicoid grass in relation to leaf position and section and environmental conditions. Plant Biol 14: 596–604.

Jafari S, Saeidnia S, Reza M, Ardekani S, Hadjiakhoondi A, Khanavi M (2013). Micromorphological and preliminary phytochemical studies of *Azadirachta indica* and *Melia azedarach*. Turk J Bot 37: 690–697.

Juggins S (2007). C2 Version 1.5 User Guide. Software for Ecological and Palaeoecological data Analysis and Visualisation. Newcastle upon Tyne, UK: Newcastle University.

Lindstrom LI, Boo BM, Mujica MB, Lutz EE (2000). Silica bodies in perennial grasses of the southern District of the Calden in central Argentina. Phyton Int J Exp Bot 69: 127–135.

Lisztes-Szabó Zs, Kovács Sz, Barna Cs (2013). Pázsitfű mellékhajtások fitolitkészletének egyedi varianciája a *Poa pratensis* L. (*Poaceae*) példáján. Bot Közl 100: 155–175 (in Hungarian).

Madella M, Alexandre A, Ball T (2005). International Code for Phytolith Nomenclature 1.0. Ann Bot-London 96: 253–260.

Madella M, Lancelotti C, Osterrieth M, editors (2012). Comprehensive perspectives on phytolith studies in Quaternary research. Quatern Int 287: 180.

Mejia-Saules T, Bisby FA (2003). Silica bodies and hooked papillae in lemmas of *Melica* species (*Gramineae*: *Pooideae*). Bot J Linn Soc 141: 447–463.

Mercader J, Astudillo F, Barkworth M, Bennett T, Esselmont C, Kinyanjui R, Grossman DL, Simpson S, Walde D (2010). *Poaceae* phytoliths from Niassa Rift, Mozambique. J Archaeol Sci 37: 1953–1967.

Mercader J, Bennett T, Esselmont C, Simpson S, Walde D (2009). Phytoliths in woody plants from the Miombo woodlands of Mozambique. Ann Bot-London 104: 91–113.

Metcalfe CR (1960). Anatomy of the Monocotyledons I. *Gramineae*. Oxford, UK: Clarendon Press.

Monsen SB, Stevens R, Shaw NL (2004). Restoring Western Ranges and Wildlands. USDA Forest Service, Rocky Mountain Research Station. General Technical Report. RMRS GTR 136: 295–698.

Morris LR, Baker FA, Morris C, Ryel RJ (2009). Phytolith types and type-frequencies in native and introduced species of the sagebrush steppe and pinyon–juniper woodlands of the Great Basin, USA. Rev Palaeobot Palyno 157: 339–357.

Mostafavi G, Assadi M, Nejadsattari T, Sharifnia F, Mehregan I (2013). Seed micromorphological survey of the *Minuartia* species (Caryophyllaceae) in Iran. Turk J Bot 37: 446–454.

Mulholland SC (1989). Phytolith shape frequencies in North Dakota Grasses: a comparison to general patterns. J Archaeol Sci 16: 489–511.

Mulholland SC, Rapp G, Ollendorf AL (1988). Variation in phytoliths from corn leaves. Can J Bot 66: 2001–2008.

Mulholland SC, Rapp G, Ollendorf AL, Regal R (1990). Variation in phytoliths within a population of corn (Mandan Yellow Flour). Can J Bot 68: 1638–1645.

Nassar MAA, Ramadan HRH, Ibrahim HMS (2013). Anatomical structures of vegetative and reproductive organs of *Senna occidentalis* (Caesalpiniaceae). Turk J Bot 37: 542–552.

Nawazish S, Hameed M, Naurin S (2006). Leaf anatomical adaptations of *Cenchrus ciliaris* L. from the Salt Range, Pakistan against drought stress. Pak J Bot 38: 1723–1730.

Peleg Z, Saranga Y, Fahima T, Aharoni A, Elbaum R (2010). Genetic control over silica deposition in wheat awns. Physiol Plant 140: 10–20.

Piperno DR, Pearsall DM (1998). The silica bodies of tropical American grasses: morphology, taxonomy, and implications for grass systematics and fossil phytolith identification. Smithsonian Contributions to Botany, Number 85. Washington, USA: Smithsonian Institution Press.

Ponzi R, Pizzolongo P (2003). Morphology and distribution of epidermal phytoliths in *Triticum aestivum* L. Plant Biosyst 137: 3–10.

Portillo M, Ball T, Manwaring J (2006). Morphometric analysis of inflorescence phytoliths produced by *Avena sativa* L. and *Avena strigosa* Schreb. Econ Bot 60: 121–129.

Premathilake R (2006). Relationship of environmental changes in central Sri Lanka to possible prehistoric land-use and climate changes. Palgeog Palclim Palecol 240: 468–496.

Prychid CJ, Rudall PJ, Gregory M (2004). Systematics and biology of silica bodies in Monocotyledons. Bot Rev 69: 377–440.

Rovner I, Russ JC (1992). Darwin and design in phytolith systematics: morphometric methods for mitigating redundancy. In: Mulholland SC, Rapp GR, editors. Phytolith Systematics: Emerging Issues. New York, NY, USA: Plenum Press.

Rudall PJ (1994). Anatomy and systematic of Iridaceae. Bot J Linn Soc 114: 1–21.

Sangster AG, Williams SE, Hodson MJ (1997). Silica deposition in the needles of the Gymnosperms. II Scanning electron microscopy and X-ray microanalysis. In: Pinilla A, Juan-Tresserras J, Machado MJ, editors. The State-of-the-Art of Phytoliths in Soils and Plants. Centro de Ciencas Medioambientales. CSIC Monograf 4: 135–146.

Soó R (1973). A Magyar flóra és vegetáció rendszertani—növényföldrajzi kézikönyve V. Budapest, Hungary: Akadémiai Kiadó, pp. 313–316 (in Hungarian).

Strömberg CAE, Werdelin L, Friis EM, Saraç G (2007). The spread of grass-dominated habitats in Turkey and surrounding areas during the Cenozoic: phytolith evidence. Palgeog Palclim Palecol 250: 18–49.

Szabo KZs, Papp M, Daroczi L (2006). Ligule morphology and anatomy of five *Poa* species. Acta Biol Crac 48: 83–88.

Tutin TG, Heywood VH, Burges NA, Moore DM, Valentine DH, Walters SM, Webb DA (1980). Flora Europaea. volume 5. Cambridge, UK: Cambridge University Press, pp. 159–162.

Twiss PC, Suess CE, Smith RM (1969). Morphological classification of grass phytoliths. Soil Sci Soc Am Proc 33: 109–115.

Wilding LP, Smeck NE, Drees LR (1977). Silica in soils: quartz, cristobalite, tridymite and opal. In: Dixon JB, Weed SB, editors. Minerals in Soil Environments. Madison, WI, USA: Soil Sci Soc Am Proc, pp. 471–552.

Yost CL, Blinnikov MS (2011). Locally diagnostic phytoliths of wild rice (*Zizania palustris* L.) from Minnesota, USA: comparison to other wetland grasses and usefulness for archaeobotany and paleoecological reconstructions. J Archaeol Sci 38: 1977–1991.

Zucol AF, Brea M, Scopel A (2005). First record of fossil wood and phytolith assemblages of the Late Pleistocene in El Palmar National Park (Argentina). J South Am Earth Sci 20: 33–43.